Proceedings of the 9th International Workshop
on Robot Motion and Control, Wasowo Palace,
Wasowo, Poland, July 3-5, 2013

Opening a door with a redundant impedance controlled robot

Tomasz Winiarski and Konrad Banachowicz*

Abstract— **Opening a door with a robotic manipulator equipped with a gripper, is a vital problem in service robotics research. This paper presents an approach to opening a cabinet door with an impedance controlled 7-DOF redundant manipulator. A control system is developed that considers redundancy in order to maximise the manipulation capabilities of the manipulator whilst avoiding reaching the joints limits. The control strategy is based on automatically estimating the kinematic parameters of the door. All conducted experiments were based on the assumption that the manipulator pulls a handle and opens a door using a single finger.**

I. INTRODUCTION

Opening a door is a vital task of a service robot, and to this date a large amount of research has been conducted in this field. Appropriate strategies involving the robot and a human operator are required to perform this task. Human operators have an advantage in this area, as they are able to evaluate the door properties based on their previous experience and can choose the opening strategy before commencing the task. Analogous research has been conducted when analysing a human operator opening a drawer [1]. Door opening strategies consist of the evaluation of an initial kinematic chain configuration before the motion is started, grip generation and execution and the formation of a motion generation strategy involving the radius vector and desired opening angle of the door. During the opening of the door, this strategy is modified in order to account for changes in the desired velocity due to the re–estimation of the inertia and frictional forces at play on the door. This results in the formulation of a real time trajectory of the movement of the door handle in the first stage of the motion. One of the first research papers conducted in this field dealt with a robot opening a door using a four degree of freedom manipulator [2]. The manipulator exerted a desired force set in the gripper tool, and the system simultaneously measured the end–effector position. The control law parameters were chosen to generate the desired force that opened the door, taking into account the trajectory of the end–effector.

Opening a door situated between rooms is an important problem for mobile robots performing indoor navigation. The main goal of this task it to let the whole robot move through a door without becoming jammed, hence a mobile base typically cooperates with a manipulator to push the door open whilst the robot navigates through the door frame. The work in [3] presents a mobile robotic system with a manipulation subsystem that is indirectly controlled from the readings of force sensors located in the gripper phalanges, as opposed to those acquired from a six-axis sensor typically mounted in the manipulator wrist [4].

The limitations of 6-DOF manipulators were part of the rationale to develop redundant manipulators [5]. The main advantages of redundant manipulators include the increase of the workspace, the introduction of higher manipulation capabilities, the possibility to work with a particular joint blocked as a 6-DOF manipulator and the possibility to avoid obstacles in the path of a kinematic chain whilst the end–effector is in motion. A serial redundant manipulator is kinematically much closer to a human arm that a 6-DOF serial manipulator. Humans successfully exploit redundancy in their arms in everyday activities, and redundant manipulators are expected to be adequate for operation in the human environment. This similarity is a reason why redundant manipulators currently dominate service robotic research.

As research in the movement of a robot through a door progresses, modern mobile manipulation platforms typically utilise redundant serial manipulators. The paper [6] presents the second version of a DLR manipulator mounted on an omni-directional mobile base. The DLR arm has torque controllers in the joints in order to maintain the desired torque. The system was designed so that when the robot moved past the door hinge, the door was kept at a distance by the impedance controlled arm.

However, the approach to door opening with mobile base motion utilisation has many disadvantages, and it is not desirable if the robot is not commanded to move from one room to another. The mobile base consumes a large amount of energy when the whole robot is in motion, especially in the case of an energetically autonomous robot equipped with heavy batteries. Moreover, the mobile base motion is slow and relatively imprecise. In some situations it can be impossible to move the robot base if there are insurmountable obstacles on the ground. Considering this, especially for the opening of a smaller door, manipulators can be used without mobile base cooperation. The 7-DOF robot described in [7] has an indirect control structure, however in this case the force readings were based on the fusion of measurements from a six-axis transducer placed in the manipulator write and force data from two gripper phalanges tactile sensors. The paper [8] concentrates on the door and hinge detection as well as kinematic estimation, but no details of the control system are presented.

II. CONTRIBUTION

In previous works [9] of the authors of this paper, a safe door opening strategy was investigated for the system of an

*Institute of Control and Computation Engineering, Warsaw University of Technology, ul. Nowowiejska 15/19, 00–665 Warsaw, Poland, tmwiniarski@gmail.com, konradb3@gmail.com

impedance controlled manipulator in rigid contact with door (analogous to [8], [7], but for a stiffer contact). This work was conducted in order to verify the approach in terms of stability and safety regarding the appearance of unexpected obstacles during the execution of the motion. For this current paper, a door opening method that uses a single finger to maintain contact with the door handle has been studied. The initial observation of a representative group of people demonstrated that opening a cabinet door with a vertical, longitudinal handle was typically achieved by using one or two fingers. The ends of the fingers were placed beneath the vertical bar of the handle and used to pull the door open - in some cases the thumb was used to stabilise the grip and increase contact stiffness, but this action was not critical for success.

The experimental results presented in this paper positively verified the proposed approach to opening a cabinet door. They were conducted for an impedance controlled, redundant manipulator without the use of a contrary thumb to grasp the handle. This strategy is versatile and can be applied not only to systems with anthropomorphic robotic grippers that are able to hold a handle from both sides, but also to manipulators without a gripper equipped with a simple tool such as a hook, and for manipulators with grippers that are in practice unable to perform the full grip with contrary thumb on small objects such as thin bars.

Previous investigation into software development for robots performing service tasks has been carried out [10], [11], as well as investigation into algorithms performing image acquisition and analysis [12] that are able to detect objects such as doors and door handles [13]. Measurements from camera and distance sensors [14] are able to support these detection algorithms. In this paper the authors concentrate on the control system synthesis for a manipulator in contact with a door handle during the door opening motion. The problem in redundant robot supervision is the adequate control of particular joints in the context of a task specified in the tool frame. Algorithms have been proposed [15] for such manipulators to both increase the manipulation capabilities whilst avoiding configuration limitations. Our approach utilises control algorithms that benefit from manipulator redundancy in order to perform the task in such a way that is unobtainable for 6-DOF manipulators. The motion strategy that is defined in the control subsystem is positioned over the lower level redundant manipulator control. It initially identifies the kinematic model parameters of the door whilst the manipulator starts to pull on the door. Following this initial identification, this process is repeatedly performed in order to correct the designed trajectory and maintain constant contact with the door handle.

This paper is organised in the following sections. Section III presents the overall system structure and control law for particular joints. The following two sections: IV and V present the medium level manipulator control, especially how it considers redundancy. The door opening strategy itself as part of control subsystem is shown in section VI. Experiments that verify the approach are illustrated in section VII. Section VIII concludes the study.

III. SYSTEM OVERVIEW

The whole system was developed as a single embodied agent due to the methodology presented in [16]. It consists of a KUKA LWR4+ manipulator with the controller herein referred to as a Real Effector, real-time control system referred to as a Virtual Effector and task execution algorithm referred to as a Control Subsystem.

The dynamic model of the system can be formulated as follows [17]:

$$\boldsymbol{M}(\boldsymbol{q})\ddot{\boldsymbol{q}}+\boldsymbol{C}(\boldsymbol{q},\ddot{\boldsymbol{q}})\dot{\boldsymbol{q}}+\boldsymbol{d}(\boldsymbol{q},\ddot{\boldsymbol{q}})+\boldsymbol{g}(\boldsymbol{q})=\boldsymbol{\tau}_r-\boldsymbol{J}^T(\boldsymbol{q})\boldsymbol{F}, \quad (1)$$

where $\boldsymbol{M}$ is the 7×7 manipulator inertia, $\boldsymbol{q}$, $\dot{\boldsymbol{q}}$, $\ddot{\boldsymbol{q}}$ are the 7×1 measured joint positions, velocities and accelerations, $\boldsymbol{C}\dot{\boldsymbol{q}}$ is the 7×1 vector of Coriolis and centrifugal torques, $\boldsymbol{d}$ is the 7×1 vector of friction torqes, $\boldsymbol{g}$ is the 7×1 vector of gravitational torques, $\boldsymbol{\tau}_r$ is the 7×1 vector of torques commanded to joint torque controllers, $\boldsymbol{J}^T$ is the 6×7 transposed Jacobian of the manipulator, and $\boldsymbol{F}$ is the 6×1 vector of contact forces exerted by the end–effector to the environment.

The Real Effector operates in joint impedance mode with its control law executed according to the formula:

$$\begin{aligned}\boldsymbol{\tau}_r[Nm]=\mathbf{K}_j\left[\frac{Nm}{rad}\right]\Delta\boldsymbol{q}[rad]-\\ \boldsymbol{D}_j\left[\frac{Nm}{rad\ s}\right]\dot{\boldsymbol{q}}\left[\frac{rad}{s}\right]+\boldsymbol{\tau}_{add}[Nm]+\boldsymbol{f}(\boldsymbol{q},\dot{\boldsymbol{q}},\ddot{\boldsymbol{q}})[Nm],\end{aligned} \quad (2)$$

where $\boldsymbol{K}_j$ is the 7×7 diagonal matrix of stiffness, $\Delta\boldsymbol{q}=\boldsymbol{q}_d-\boldsymbol{q}$ is the 7×1 deflection of a virtual spring, $\boldsymbol{q}_d$ is a 7×1 desired joint position, $\boldsymbol{D}_j$ is the 7×7 diagonal matrix of damping, $\boldsymbol{\tau}_{add}$ is an additional 7×1 input torque and $\boldsymbol{f}$ is robot dynamics supplemented by gravity compensation. Joint level impedance regulators operate at 3kHz frequency and joint torque controllers operate at tens of kHz. The structure of this regulator as well as its stability analysis were presented in [18].

The Real Effector communicates with the Virtual Effector using an FRI[1] [19] interface which enables real-time control of the manipulator from an external PC. At every communication cycle of the FRI (1 ms) values of $\boldsymbol{K}_j$, $\boldsymbol{D}_j$, $\boldsymbol{q}_d$ and $\boldsymbol{\tau}_{add}$ are sent to the Real Effector. The Virtual Effector implements a high level real-time controller for an arm and provides convenient interfaces for task implementation in the Control Subsystem (sec. VI). Due to the redundancy of the arm, the Virtual Effector executes two complementary sets of control algorithms herein referred to as a Primary Subtask and a Secondary Subtask.

The resulting commanded torque $\boldsymbol{\tau}_{add}$ is the sum of corresponding torques from primary $\boldsymbol{\tau}_p$ and secondary $\boldsymbol{\tau}_S$ subtasks. The Primary Subtask (sec. IV) realises Cartesian impedance control and end-effector trajectory generation, whereas the Secondary Subtask (sec. V) contains the set of algorithms controlling the nullspace motion of the arm to maximally exploit manipulation capabilities.

[1]Fast Research Interface

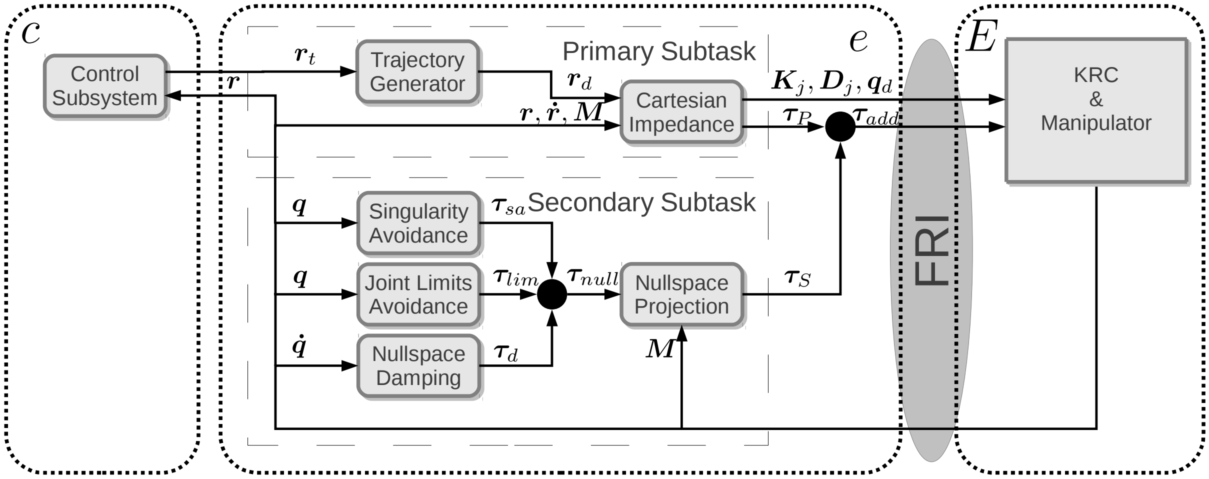

Fig. 1. System diagram: c – Control Subsystem (ROS programming framework running on PC computer), e – Virtual Effector (OROCOS programming framework running on PC computer), E – Real Effector (KUKA Robot Controller running on PC computer and LWR4+ manipulator)

IV. CARTESIAN IMPEDANCE ENHANCED BY LOCAL STIFFNESS CONTROL

The impedance control has the advantage of being able to incorporate door opening tasks in a larger application consisting of multiple stages. This is achieved by adjusting the impedance characteristics for the smooth transition of the motion without any contact of the manipulator with the environment to the contact phase, as is obtainable in pneumatic-driven robots [20].

The impedance controller used in this work is composed of:

- Direct impedance controller (sec. IV-A) which is directly derived from impedance equations and provides exact realisation of commanded impedance.
- Local stiffness controller (sec. IV-B) which exploits higher bandwidth of joint impedance controllers and this way increases the feasible range of stiffness.

A. Direct Impedance Controller

The desired 6×1 force $\boldsymbol{F}_d$ at the tool frame is calculated (3) as a superposition of forces originating from a virtual spring and damper. The stiffness component is calculated by taking into account the 6×6 Cartesian stiffness matrix $\boldsymbol{K}_c$ and the 6×1 virtual spring displacement $\Delta \boldsymbol{r}$ [21] between measured position $\boldsymbol{r}$ (consisting of 3×1 position vector supplemented by a unit quaterion) and commanded equilibrium point $\boldsymbol{r}_d$ represented in the same way:

$$\boldsymbol{F}_d = \boldsymbol{K}_c \Delta \boldsymbol{r} - \boldsymbol{D}_c(\boldsymbol{q}, \boldsymbol{\xi}) \dot{\boldsymbol{r}}, \tag{3}$$

$$\boldsymbol{\tau}_P = \boldsymbol{J}^T(\boldsymbol{q}) \boldsymbol{F}_d \; . \tag{4}$$

In general, the position $\boldsymbol{r}$ in terms of $\boldsymbol{q}$ is computed using direct kinematics. Trajectory generation provides target equilibrium points $\boldsymbol{r}_d$ for the impedance controller by interpolating between the trajectory points $\boldsymbol{r}_t$ (using linear interpolation for position and spherical interpolation for rotation). The damping term is composed of a 6×6 configuration dependent damping matrix $\boldsymbol{D}_c$ and 6×1 the velocity of the tool frame $\dot{\boldsymbol{r}}$. The damping matrix is calculated at every control cycle using the double-diagonalisation [22] method and is parametrised by $\boldsymbol{\xi}$ 6×1 a vector representing normalised damping along the main directions of the task frame. Following this, the tool frame force is transformed (4) into joint torques by 6×7 the transposed Jacobian $\boldsymbol{J}^T$ of the manipulator.

B. Local Stiffness Control

Desired impedance behaviour is achieved by projecting Cartesian stiffness K_c into joint space:

$$\boldsymbol{K}_j \quad = \quad \boldsymbol{J}^T(\boldsymbol{q}) \boldsymbol{K}_c \boldsymbol{J}(\boldsymbol{q}) \; . \tag{5}$$

The resulting joint stiffness matrix $\boldsymbol{K}_j$ is only valid locally and, because of the decentralised architecture of the joint controllers, only the diagonal part of this matrix can be used. The joint equilibrium point is set as the measured position of the joint at every FRI communication cycle and this way $\boldsymbol{K}_j$ only locally affects the joint torque. A more detailed description of this control scheme can be found in [23]. All of the elements of the joint space damping matrix $\boldsymbol{D}_j$ are set to zero, as joint damping cannot be applied locally.

V. NULLSPACE BEHAVIOUR

It is essential when performing Cartesian impedance control to not impinge on the mechanical limits of the joints and to avoid singular configurations. The Secondary Subtask that realises the nullspace control is composed of three components, presented later in this paper, that generate three torques: $\boldsymbol{\tau}_{lim}$, $\boldsymbol{\tau}_{sa}$ and $\boldsymbol{\tau}_d$. These torques are summed (7) and then transformed through a projection matrix $\mathcal{N}$:

$$\mathcal{N}(\boldsymbol{J}) = \boldsymbol{I} - \boldsymbol{J}^T (\boldsymbol{J}^+)^T, \tag{6}$$

$$\boldsymbol{\tau}_{null} = \boldsymbol{\tau}_{lim} + \boldsymbol{\tau}_{sa} + \boldsymbol{\tau}_d, \tag{7}$$

$$\boldsymbol{\tau}_S = \mathcal{N}\big(\boldsymbol{J}(q)\big) \boldsymbol{\tau}_{null}, \tag{8}$$

where $\boldsymbol{J}^{+}$ is the pseudo-inverse of the Jacobian:

$$\boldsymbol{J}^{+\boldsymbol{A}} = \boldsymbol{A}\boldsymbol{J}^{T}(\boldsymbol{J}\boldsymbol{A}\boldsymbol{J}^{T})^{-1}. \tag{9}$$

By replacing matrix A with the inverse of manipulator inertia $\boldsymbol{M}$, the dynamically consistent projection matrix is obtained [24].

A. Joint Limits Avoidance

To avoid reaching the mechanical limits of the joints, unilateral virtual springs have been constructed around the positions of these limits:

$$V_{par}(z_c, z_g, z_d) = \begin{cases} k_l(z_c - z_g)^2 & z_c > z_g \\ 0 & z_c \in \langle z_d, z_g \rangle \\ k_l(z_c - z_d)^2 & z_c < z_d, \end{cases} \tag{10}$$

where k_l is a proportionality factor, z_c is the current value, z_g is the upper limit and z_d is the lower limit. A potential function V_{lim} can then be computed:

$$V_{lim}(\boldsymbol{q}, \boldsymbol{q}_{max}, \boldsymbol{q}_{min}) = \sum_{l=1}^{n} V_{par}(\boldsymbol{q}_{[l]}, \boldsymbol{q}_{max[l]}, \boldsymbol{q}_{min[l]}), \tag{11}$$

where n is the number of joints ($n = 7$ for KUKA LWR4+), $\boldsymbol{q}_{min}$ is the lower joints limit and $\boldsymbol{q}_{max}$ is the upper joints limit. The right subscript in square brackets determines the particular coordinate of the vector. The corresponding torque $\boldsymbol{\tau}_{lim}$ is calculated as a gradient of the potential function $V_{lim}(\boldsymbol{q})$:

$$\boldsymbol{\tau}_{lim} = -\frac{\partial V_{lim}(\boldsymbol{q})}{\partial \boldsymbol{q}} . \tag{12}$$

B. Singularity Avoidance

To detect the proximity of a singular configuration, a manipulability function (13) is used, as defined by Yoshikawa [25]:

$$m(\boldsymbol{q}) = \sqrt{\det\left(\boldsymbol{J}(\boldsymbol{q})\boldsymbol{J}^{T}(\boldsymbol{q})\right)} . \tag{13}$$

The potential function $V_{sa}(\boldsymbol{q})$ is constructed:

$$V_{sa}(\boldsymbol{q}) = \begin{cases} k_s\left(m(\boldsymbol{q}) - m_0\right)^2 & m(\boldsymbol{q}) \leq m_0 \\ 0 & m(\boldsymbol{q}) > m_0, \end{cases} \tag{14}$$

where m_0 is the manipulability threshold value. The resulting torque $\boldsymbol{\tau}_{sa}$ is calculated as the gradient of the potential function:

$$\boldsymbol{\tau}_{sa} = -\frac{\partial V_{sa}(\boldsymbol{q})}{\partial \boldsymbol{q}} . \tag{15}$$

C. Nullspace Damping

Dampening in joint space is introduced to ensure that no undesirable nullspace oscillations build up:

$$\boldsymbol{\tau}_d = -\boldsymbol{D}_0\dot{\boldsymbol{q}}, \tag{16}$$

where $\boldsymbol{D}_0$ is an arbitrary positive definite damping matrix and $\boldsymbol{\tau}_d$ represents the respective torques.

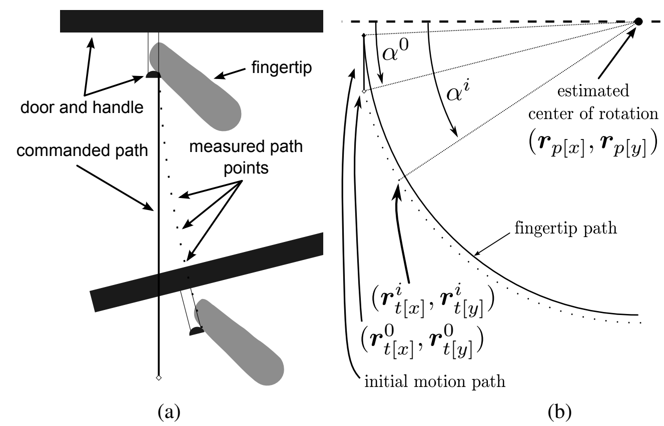

Fig. 2. Door opening algorithm: (a) – initial motion (b) – trajectory generation

VI. Door Opening Algorithm

The proposed algorithm of opening a door is composed of two steps: the first provides an initial estimation of the door kinematics and the second executes the compliant trajectory.

A. Initial Estimation of Door Kinematics

An initial estimation of the door kinematic parameters is achieved by moving the tool equilibrium point along a linear trajectory (Fig. 2a) and collecting the measured positions of the fingertip. Assuming that the axis of rotation of the door is parallel to the world Z axis, the kinematics parameters are estimated by fitting a circle into measured points along the fingertip path in the XY plane. The circle fitting is done using a least-squares method to compute both the radius p^i and centre of rotation $(\boldsymbol{r}_{p[x]}, \boldsymbol{r}_{p[y]})$. The right subscript in square brackets determines the coordinates of the reference coordinate system, where the translational components are labelled by x, y and z. When an initial estimation is available, an angle α^0 is calculated:

$$\alpha^0 = atan2(\boldsymbol{r}^0_{t[y]} - \boldsymbol{r}^0_{p[y]}, \boldsymbol{r}^0_{t[x]} - \boldsymbol{r}^0_{p[x]}), \tag{17}$$

where $(\boldsymbol{r}^0_{p[x]}, \boldsymbol{r}^0_{p[y]})$ is the centre of rotation from the initial estimation, $(\boldsymbol{r}^0_{t[x]}, \boldsymbol{r}^0_{t[y]})$ is the equilibrium point (desired position) at the end of initial motion (Fig. 2b).

B. Compliant Trajectory Execution

In the second phase, the control system generates short trajectory segments along the estimated handle path. For every trajectory segment α^i is calculated (18) and the corresponding points on the XY plane are calculated (19, 20).

$$\alpha^i = \alpha^0 + i \cdot \alpha_{step}, \tag{18}$$

$$\boldsymbol{r}^{i+1}_{t[x]} = \sin\left(\alpha^{i+1}\right)(p^i + p_{ext}) + \boldsymbol{r}^i_{p[x]}, \tag{19}$$

$$\boldsymbol{r}^{i+1}_{t[y]} = \cos\left(\alpha^{i+1}\right)(p^i + p_{ext}) + \boldsymbol{r}^i_{p[y]} . \tag{20}$$

The estimated radius p^i is extended by p_{ext} to generate a force that keeps the contact with the door's handle. The resulting trajectory segment is composed of translations $(\boldsymbol{r}^i_{d[x]}, \boldsymbol{r}^i_{d[y]})$ and a rotation around Z axis α^i. The remaining coordinates remain constant from the beginning of the motion. During the execution of the segment a new measurement of fingertip pose is completed and the circle fitting is repeated whereby the new parameters of the door kinematics are available for the next trajectory segment. The trajectory generation routine is repeated until a desired angle of rotation is achieved. An advantage of the impedance control is that there is no need to measure the forces in the end–effector for the presented strategy of door opening. The force exerted on the door handle is dependant on the $\boldsymbol{K}_c$ stiffness, defined in Cartesian coordinates, and the p_{ext} radius extension.

VII. Experimental Results

In the experiments, the manipulator tool took the form of a single BarrettHand finger. There was no visual feedback and no wrist force sensor was used. Torques were measured directly in the joints for the purpose of joint torque control, and the wrist general force was computed internally by the KUKA LWR controller.

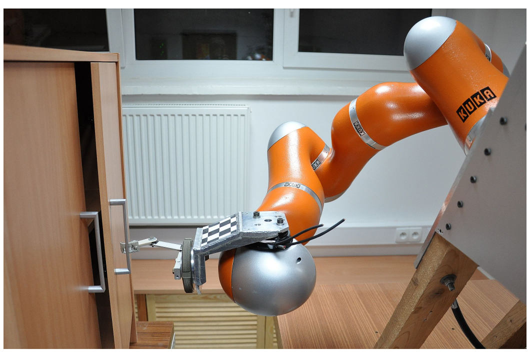

Fig. 3. Experimental setup – front view

The proposed algorithm has been evaluated by opening the cabinet door with the handle located at various radii from the door hinge (Fig. 3). Both the $\boldsymbol{K}_c$ and the p_{ext} values were changed to investigate the system properties. The $\boldsymbol{K}_c$ linear coordinates were changed from $200\frac{\mathrm{N}}{\mathrm{m}}$ to $1000\frac{\mathrm{N}}{\mathrm{m}}$ as well as p_{ext} values from 0.005m to 0.02m. It was found that for the above parameter values, the system was robust and the operation success depended mainly on the quality of the motion that preceded the door opening itself. The excessive increase of controller stiffness $\boldsymbol{K}_c$ and radius enlargement p_{ext} led to the generation of undesirably large contact forces. At the other extreme, the low values of $\boldsymbol{K}_c$ and p_{ext} caused the loss of contact.

TABLE I
Commanded Values for the Cartesian Stiffness Matrix

x	y	z	roll	pitch	yaw
1000.0 $\frac{\mathrm{N}}{\mathrm{m}}$	200.0 $\frac{\mathrm{N}}{\mathrm{m}}$	1000.0 $\frac{\mathrm{N}}{\mathrm{m}}$	200.0 $\frac{\mathrm{Nm}}{\mathrm{rad}}$	200.0 $\frac{\mathrm{Nm}}{\mathrm{rad}}$	200.0 $\frac{\mathrm{Nm}}{\mathrm{rad}}$

An exemplary experiment series is shown which is additionally presented in a movie[2]. The series consisted of the opening of the door with the handle located in three different places with various radii from hinge. The impedance properties of the end-effector were set as shown in table I, the value of p_{ext} was set to 0.01m and the initial trajectory was 0.1m motion along the direction of vector normal to the door plane. All parameters remained unchanged for the whole series of the experiment.

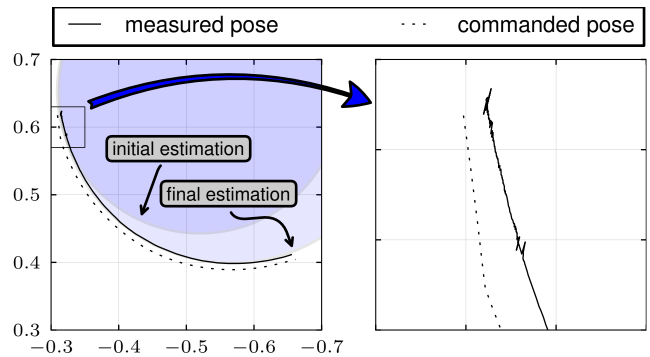

Fig. 4. Experiment for large radius (scaled in meters)

As shown in Fig. 4 and Fig. 5 the initial estimation underestimated the door handle radius. The source of this effect has not been found – the estimation is affected by multiple variables including errors in modelling of the tool geometry, uncertainty of the location of the contact points between fingertip and handle, errors in the door kinematics modelling and numerical errors. Despite the errors introduced by the initial estimation, the impedance controller performed well at keeping the fingertip in contact with the handle. During the motion, more data became available to analyse, and the estimation improved significantly before stabilising.

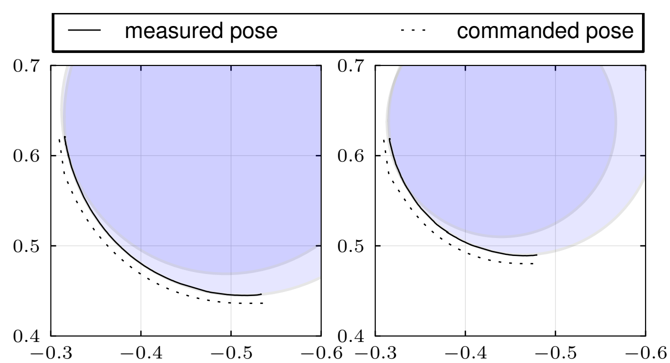

Fig. 5. Experiments for medium and small radius (scaled in meters)

Fig. 6 presents the forces generated on the handle during the exemplary experiment. It was found that the forces did not change rapidly and were within acceptable ranges in order to prevent handle damage.

VIII. Conclusions

The proposed system is able to open a door by pulling the handle with a single finger. The approach has been

[2]http://vimeo.com/rcprg/door-opening-with-finger

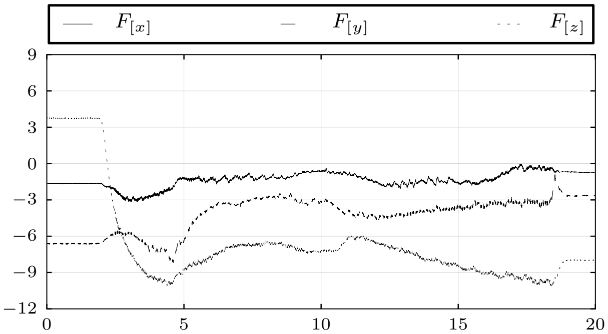

Fig. 6. Forces measured in tool during task execution.

formally specified, presented and verified experimentally by an impedance controlled KUKA-LWR4+ manipulator with a custom built, research-oriented control system. Future work will utilise the upcoming manipulation system enhancements. The first of these is a rotating body intended for further extension of the manipulation capabilities and manipulation workspace. The second consists of the introduction of tactile sensors mounted on the fingertips, which can be used for contact verification in the initial phase of the motion. These modifications will allow opening of larger doors than investigated thus far, and will increase the overall system robustness.

ACKNOWLEDGMENT

This project was funded by the National Science Centre according to the decision number DEC-2012/05/D/ST6/03097. Tomasz Winiarski has been supported by the European Union in the framework of the European Social Fund through the Warsaw University of Technology Development Programme. The authors thank Eloise Matheson for her help in the paper editing.

REFERENCES

[1] D. Serrien and M. Wiesendanger, "Grip-load force coordination in cerebellar patients," *Experimental brain research*, vol. 128, no. 1, pp. 76–80, 1999.

[2] G. Niemeyer and J. Slotine, "A simple strategy for opening an unknown door," in *International Conference on Robotics and Automation (ICRA)*, vol. 2. IEEE, 1997, pp. 1448–1453.

[3] W. Chung, C. Rhee, Y. Shim, H. Lee, and S. Park, "Door-opening control of a service robot using the multifingered robot hand," *IEEE Transactions on Industrial Electronics*, vol. 56, no. 10, pp. 3975–3984, 2009.

[4] T. Winiarski and A. Woźniak, "Indirect force control development procedure," *Robotica*, vol. 31, pp. 465–478, 4 2013.

[5] R. Bischoff, J. Kurth, G. Schreiber, R. Koeppe, A. Albu-Schäffer, A. Beyer, O. Eiberger, S. Haddadin, A. Stemmer, G. Grunwald, *et al.*, "The kuka-dlr lightweight robot arm-a new reference platform for robotics research and manufacturing," in *41st International Symposium on Robotics (ISR) and 6th German Conference on Robotics (ROBOTIK)*. VDE, 2010, pp. 1–8.

[6] C. Ott, B. Bäuml, C. Borst, and G. Hirzinger, "Employing cartesian impedance control for the opening of a door: A case study in mobile manipulation," in *IEEE/RSJ international conference on intelligent robots and systems workshop on mobile manipulators: Basic techniques, new trends & applications*, 2005.

[7] A. Schmid, N. Gorges, D. Goger, and H. Worn, "Opening a door with a humanoid robot using multi-sensory tactile feedback," in *International Conference on Robotics and Automation (ICRA)*. IEEE, 2008, pp. 285–291.

[8] T. Ruhr, J. Sturm, D. Pangercic, M. Beetz, and D. Cremers, "A generalized framework for opening doors and drawers in kitchen environments," in *International Conference on Robotics and Automation (ICRA)*. IEEE, 2012, pp. 3852–3858.

[9] T. Winiarski, K. Banachowicz, and M. Stefańczyk, "Safe strategy of door opening with impedance controlled manipulator," *Journal of Automation Mobile Robotics and Intelligent Systems*, 2013, (accepted for publication).

[10] T. Winiarski and C. Zieliński, "Specification of multi-robot controllers on an example of a haptic device," in *Robot Motion and Control (LNCiS) Lecture Notes in Control & Information Sciences*, K. Kozłowski, Ed., vol. 396. Springer Verlag London Limited, 2009, pp. 227–242.

[11] M. Quigley, B. Gerkey, K. Conley, J. Faust, T. Foote, J. Leibs, E. Berger, R. Wheeler, and A. Ng, "ROS: an open-source Robot Operating System," in *Proceedings of the Open-Source Software workshop at the International Conference on Robotics and Automation (ICRA)*, 2009.

[12] T. Kornuta, T. Bem, and T. Winiarski, "Utilization of the FraDIA for development of robotic vision subsystems on the example of checkers' playing robot," *Machine GRAPHICS & VISION*, 2013, (accepted for publication).

[13] M. Chacon-Murguia, R. Sandoval-Rodriguez, and C. Guerrero-Saucedo, "Fusion of door and corner features for scene recognition," *Journal of Automation Mobile Robotics and Intelligent Systems*, vol. 5, no. 1, pp. 68–76, 2011.

[14] M. Stefańczyk and W. Kasprzak, "Multimodal segmentation of dense depth maps and associated color information," in *Proceedings of the International Conference on Computer Vision and Graphics*, ser. Lecture Notes in Computer Science, vol. 7594. Springer Berlin / Heidelberg, 2012, pp. 626–632.

[15] A. Dietrich, T. Wimbock, and A. Albu-Schaffer, "Dynamic whole-body mobile manipulation with a torque controlled humanoid robot via impedance control laws," in *International Conference on Intelligent Robots and Systems (IROS)*. IEEE/RSJ, 2011, pp. 3199–3206.

[16] T. Kornuta and C. Zieliński, "Behavior-based control system of a robot actively recognizing hand postures," in *15th IEEE International Conference on Advanced Robotics, ICAR*, June 2011, pp. 265–270.

[17] S. Chiaverini, B. Siciliano, and L. Villani, "A survey of robot interaction control schemes with experimental comparison," *IEEE/ASME Transactions on Mechatronics*, vol. 4, no. 3, pp. 273–285, 1999.

[18] A. Albu-Schäffer, C. Ott, and G. Hirzinger, "A unified passivity-based control framework for position, torque and impedance control of flexible joint robots," *The International Journal of Robotics Research*, vol. 26, no. 1, pp. 23–39, 2007.

[19] G. Schreiber, A. Stemmer, and R. Bischoff, "The fast research interface for the kuka lightweight robot," in *IEEE ICRA Workshop on Innovative Robot Control Architectures for Demanding (Research) Applications–How to Modify and Enhance Commercial Controllers. Anchorage*, 2010.

[20] E. Jezierski and G. Granosik, "Modeling and control of jumping robot with pneumatic drive," in *13th IEEE IFAC Int. Conf. on Methods and Models in Automation and Robotics, Szczecin, Poland*, 2007, pp. 941–945.

[21] F. Caccavale, C. Natale, B. Siciliano, and L. Villani, "Six-dof impedance control based on angle/axis representations," *IEEE Transactions on Robotics and Automation*, vol. 15, no. 2, pp. 289–300, 1999.

[22] A. Albu-Schaffer, C. Ott, U. Frese, and G. Hirzinger, "Cartesian impedance control of redundant robots: Recent results with the dlr-light-weight-arms," in *International Conference on Robotics and Automation (ICRA)*, vol. 3. IEEE, 2003, pp. 3704–3709.

[23] A. Albu-Schaffer and G. Hirzinger, "Cartesian impedance control techniques for torque controlled light-weight robots," in *International Conference on Robotics and Automation (ICRA)*, vol. 1. IEEE, 2002, pp. 657–663.

[24] O. Khatib, "A Unified Approach for Motion and Force Control of Robot Manipulators: The Operational Space Formulation," *International Journal of Robotics and Automation*, vol. RA-3, no. 1, pp. 43–53, February 1987.

[25] T. Yoshikawa, "Manipulability of robotic mechanisms," *The international journal of Robotics Research*, vol. 4, no. 2, pp. 3–9, 1985.